

Monolithic Aerogels Based on Poly(2,6-diphenyl-1,4-phenylene oxide) and Syndiotactic Polystyrene

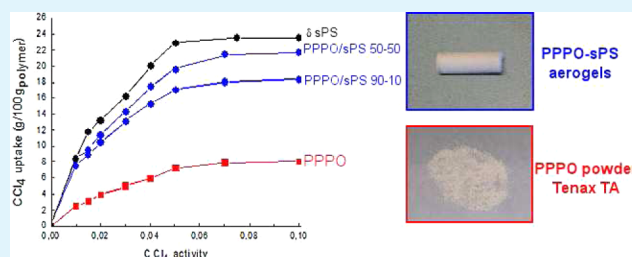
Simona Longo,[†] Jenny G. Vitillo,[‡] Christophe Daniel,^{*,†} and Gaetano Guerra[†]

[†]Dipartimento di Chimica e Biologia, INSTM Research Unit, Università degli Studi di Salerno, via Ponte Don Melillo, 84084 Fisciano (SA), Italy

[‡]Dipartimento di Chimica and NIS Centre of Excellence, Università di Torino, Via Giuria 7, Torino 10125, Italy

ABSTRACT: Molecular sorption behavior of amorphous and semicrystalline samples based on poly(2,6-diphenyl-1,4-phenylene oxide) (PPPO) has been compared. Fully amorphous PPPO powders, as obtained by supercritical carbon dioxide (scCO₂) extraction of concentrated solutions, present uptake of pollutants much higher than for commercial sorbent materials based on semicrystalline PPPO (Tenax TA). Robust monolithic aerogels with good handling characteristics can be easily obtained by solvent extraction by scCO₂ from gels including PPPO blends with syndiotactic polystyrene (s-PS). These monolithic PPPO/s-PS aerogels present many advantages as sorbent materials with respect to both amorphous and semicrystalline PPPO powders. In fact, besides the obvious advantages in terms of easier and safer handling, the new monolithic aerogels present higher surface areas and equilibrium guest uptakes.

KEYWORDS: Tenax, syndiotactic polystyrene, physical gels, aerogels, blends, sorbent materials, pollutants, X-ray diffraction



1. INTRODUCTION

Poly(2,6-diphenyl-1,4-phenylene oxide) (shortly indicated as PPPO), which was patented in 1969,¹ has been mainly developed with the trade name Tenax as a porous column packing polymer for gas chromatography.² Indeed, PPPO is an excellent porous adsorbent for the trapping of many types of volatiles such as halogenated and aromatic compounds,^{3–5} normal alkanes,^{3,6,7} cycloalkanes,³ ketones,^{3,5–7} alcohols,^{3,5–7} and volatile fatty acids⁵ mainly from air^{3,5–7} but also from water.⁴

Moreover PPPO, generally provided in granular form, has several attractive features for a use as a porous material in air analysis: it is thermally stable (up to 350 °C for Tenax TA),⁸ presents a low water retention,³ and is relatively resistant to oxygen.² Thus PPPO is largely used as an adsorbent material in standard methods for routine air monitoring⁹ or for the study of specific industrial emissions.^{10–12}

Recently, for a structurally similar polymer, poly(2,6-dimethyl-1,4-phenylene oxide) generally known as PPO, the occurrence of nanoporous-crystalline modifications exhibiting high guest solubility already for low guest activity, has been established.^{13–16} In fact, semicrystalline samples of PPO present particularly relevant transport properties, because their nanoporous-crystalline phases present guest solubilities and diffusivities even higher than those (already particularly high)^{17–22} of their amorphous phases.

Syndiotactic polystyrene (s-PS) is the only one other polymer beside PPO for which the formation of two nanoporous crystalline forms, called δ ^{23,24} and ϵ ,²⁵ has been reported in literature. As for PPO, it has also been observed for

s-PS that, for low activities, the sorption of volatile organic compounds (mainly halogenated or aromatic hydrocarbons) from air and water is higher in the nanoporous crystalline phases than in the amorphous phase.^{26,27}

Thus, as for most molecular sorption studies^{2–7,10–12} PPPO is used as a semicrystalline powder, the first aim of the present study was to establish if the occurrence of a nanoporous crystalline phase could be at the origin of the high sorption properties of PPPO.

Aerogels constitute a unique class of materials, characterized by a highly porous network making them attractive for many applications such as thermal and acoustic insulation, capacitors or catalysis.²⁸

Since the pioneering report of Pekala²⁹ it has been shown that monolithic organic based aerogels can be easily prepared from chemically cross-linked gels obtained with various polymers such as polydimethylsiloxane,³⁰ or polyimide.³¹

Monolithic and robust aerogels, have been obtained also from thermoreversible gels of crystallizable synthetic polymers^{32–36} or biopolymers,^{37–39} by sudden solvent extraction with supercritical carbon dioxide (scCO₂). The good handling characteristics and the high diffusivities due to the presence of macropores makes these monolithic aerogels very promising for water and air purification, mainly when they are based on polymers characterized by nanoporous-crystalline phases such as s-PS or PPO.^{40–47}

Received: February 15, 2013

Accepted: May 23, 2013

Published: May 23, 2013

Hence, a second aim of the present study is to explore the possibility to obtain PPPO aerogels, in the attempt to improve the already high sorption capability of this polymer.

2. EXPERIMENTAL SECTION

2.1. Material and Sample Preparation. Poly(2,6-diphenyl-1,4-phenylene oxide) used in this work was purchased from Sigma Aldrich (Tenax TA 60–80 mesh) and syndiotactic polystyrene was manufactured by Dow Chemicals under the trademark Questra 101. ^{13}C nuclear magnetic resonance characterization showed that the content of syndiotactic triads was over 98%. Weight-averaged and number-averaged molecular masses were found to be $M_w = 320\,000\text{ g mol}^{-1}$ and $M_n = 82\,000\text{ g mol}^{-1}$. Solvents were purchased from Aldrich and used without further purification.

All gel samples were prepared with chloroform in hermetically sealed test tubes by heating the mixtures at ca. $140\text{ }^\circ\text{C}$ until complete dissolution of the polymer and the appearance of a transparent and homogeneous solution had occurred. Then the hot solution was cooled down to room temperature where gelation occurred.

The total polymer concentration and the polymer weight ratio were set by weighting the solvent and both polymers. All gel samples prepared to get the aerogels were prepared at a total polymer concentration $C_{\text{pol}} = 10\text{ wt } \%$ with $C_{\text{pol}} = 100m_{\text{polymer}}/(m_{\text{polymer}} + m_{\text{solvent}})$ where m_{pol} and m_{sol} are the masses of the polymers and of the solvent, respectively using c.a. five mL of chloroform for the gel preparation.

Solvent was extracted directly from the gels with a SFX 200 supercritical carbon dioxide extractor (ISCO Inc.) putting the samples in a 10 mL cartridge. The extraction was carried out using the following conditions: $T = 40\text{ }^\circ\text{C}$, $P = 250\text{ bar}$, extraction time $t = 300\text{ min}$. The operative pressure conditions were reached in less than 1 min. During the extraction the CO_2 flow rate was set at ca. $2\text{--}3\text{ mL/min}$ and after solvent extraction the sample cartridge was slowly depressurized at a flow rate of 2 mL/min before removal from the extractor.

For monolithic aerogels with a regular cylindrical shape, the total porosity, including macroporosity, mesoporosity and microporosity, can be estimated from the mass/volume ratio of the aerogel. Then, the percentage of porosity P of the aerogel samples can be expressed as

$$P = 100 \left(1 - \frac{\rho_{\text{app}}}{\rho_{\text{pol}}} \right)$$

where ρ_{pol} is the density of the polymer matrix and ρ_{app} is the aerogel apparent density calculated from the mass/volume ratio of the monolithic aerogels.

2.2. Techniques. Wide-Angle X-ray Diffraction (WAXD). X-ray diffraction patterns were obtained on a Bruker D8 automatic diffractometer operating at a step size of 0.03° , a rate of 164 s/step and with a nickel-filtered $\text{CuK}\alpha$ radiation. Diffraction patterns of aerogels were obtained with cylinder-shaped samples, with a thickness of 2 mm .

The degree of crystallinity of the samples was evaluated from X-ray diffraction data applying the standard procedure of resolving the diffraction pattern into two areas corresponding to the contributions of the crystalline and amorphous fractions for the 2θ range $6\text{--}35^\circ$.

VOC Sorption Experiments. The VOC vapor sorption measurements have been carried out at $35\text{ }^\circ\text{C}$ with a VTI-SA symmetrical vapor sorption analyzer from TA Instruments. The equilibrium criteria used for the measurements were a weight uptake of 0.01% in 5 min with a maximum equilibrium time of 240 min .

The VOC equilibrium uptakes from diluted aqueous solutions have been determined at $20\text{ }^\circ\text{C}$ after c.a. four days of sample immersion in a 1 L solution being maintained under stirring. The weight gain of samples was obtained by thermogravimetric measurements (TGA) performed with a TG 209 F1 from Netzsch after accurate samples wiping. A 10 mL/min nitrogen flow and a $10\text{ }^\circ\text{C/min}$ heating rate were used for all the measurements.

SEM. The internal morphology of the aerogels was characterized by means of a LEO 1525 Field Emission Scanning Electron Microscope. Samples were prepared by fracturing small pieces of the monoliths in order to gain access to the internal part of the specimen. Before imaging, all the specimens were coated with gold using a VCR high resolution indirect ion-beam sputtering system. The samples were coated depositing approximately 20 nm of gold.

Porosimetry. Surface area and pore volume were obtained by N_2 adsorption measurements carried out at 77 K on a Micromeritics ASAP 2020 sorption analyzer. All the samples were outgassed for 24 h at $30\text{ }^\circ\text{C}$ before the analysis. The specific surface area of the polymers was calculated using the Brunauer–Emmet–Teller method.⁴⁸

3. RESULTS AND DISCUSSION

3.1. PPPO Powders and Films. The as-received commercial PPPO powder presents the X-ray diffraction pattern shown in Figure 1A, typical of the known crystalline phase⁷ with a degree of crystallinity close to 40% .

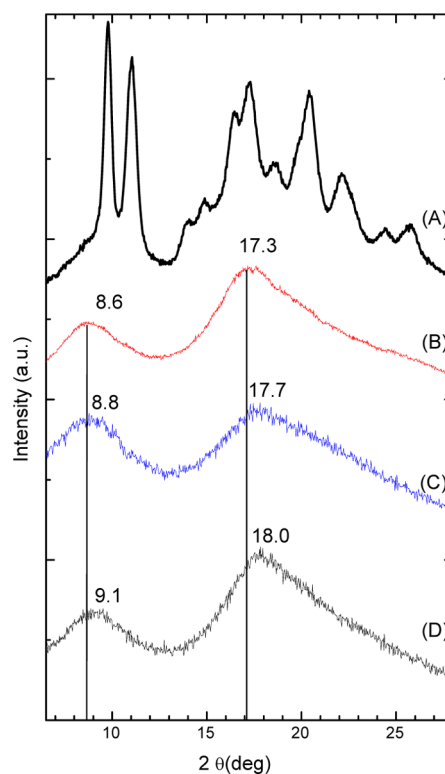


Figure 1. X-ray diffraction patterns ($\text{CuK}\alpha$ radiation) of PPPO samples: (A) as-received commercial semicrystalline powder; (B) amorphous powder, obtained by sCO_2 extraction of a concentrated solution; (C, D) amorphous films obtained by casting in CHCl_3 at (C) 135 and (D) $20\text{ }^\circ\text{C}$.

The X-ray diffraction patterns of powders obtained from a concentrated CHCl_3 solution ($C_{\text{pol}} = 20\text{ wt } \%$) by sCO_2 extraction and of films obtained by casting from CHCl_3 solutions at $135\text{ }^\circ\text{C}$ and at $20\text{ }^\circ\text{C}$, are shown in Figure 1B–D, respectively. The three patterns present the typical PPPO amorphous halo with two maxima,⁴⁹ which are however centered at definitely different 2θ values: at 8.6° and 17.3° for the sCO_2 extracted powder while in the ranges $8.8\text{--}9.1^\circ$ and $17.7\text{--}18.0^\circ$ for the films. The most dense amorphous sample (corresponding to the pattern shifted at highest 2θ values of Figure 1D) is obtained for the low temperature solution casting procedure while the less dense amorphous

sample (corresponding to the pattern shifted at lowest 2θ values of Figure 1B) is obtained for the powder obtained by sudden solvent removal by scCO_2 .

The samples of Figure 1 have been compared as sorbent materials for carbon tetrachloride (CCl_4) vapor at low activity. The choice of CCl_4 as test pollutant is related to its very slow degradation, leading to gradual accumulation in the environment.⁵⁰

Gravimetric CCl_4 sorption isotherms, at 35 °C and at activities (p/p_0) up to 0.2, are reported in Figure 2. For the

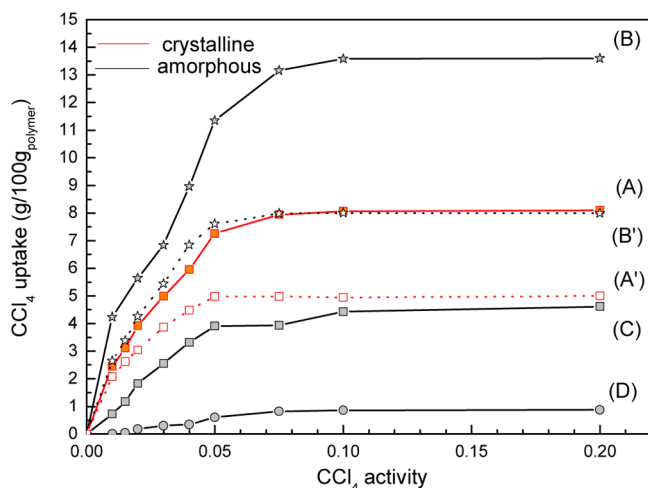


Figure 2. CCl_4 sorption isotherms at 35 °C for PPPO samples: (A) as-received commercial semicrystalline Tenax TA powder; (B) fully amorphous powder, obtained by scCO_2 extraction of a concentrated solution; (C, D) fully amorphous films obtained by casting in CHCl_3 at (C) 135 and (D) 20 °C. The dotted curves with empty symbols (A' and B') indicate the sorption isotherms of the semicrystalline and amorphous powders A and B after annealing at 220 °C.

entire CCl_4 activity range, the equilibrium uptake from the amorphous powder (Figure 2B) is much higher than from the two amorphous films (Figure 2C, D) and also higher than for the commercial semicrystalline powder (Figure 2A). For instance, the equilibrium sorption at $p/p^\circ = 0.10$ for the amorphous powder is nearly 14 wt % while for the semicrystalline powder is nearly 8 wt % and for the amorphous films cast at 135 and 20 °C is lower than 5 and 1 wt %, respectively.

The different values of the CCl_4 sorption uptake obtained with the cast films and the amorphous powder can be attributed to the different density of the amorphous phases obtained in the three samples. In fact the most dense sample (i.e., cast film prepared at 20 °C) is characterized by the lowest CCl_4 uptake (Figure 2 D) while the less dense sample (i.e., powder obtained by scCO_2 extraction of a concentrated solution) presents the highest CCl_4 uptake (Figure 2 B).

The guest uptake from the semicrystalline sample (Figure 2A), is roughly equal to 60% of the guest uptake of the amorphous powder (Figure 2B), i.e., close to the amorphous content of the semicrystalline powder. This indicates that, as generally occurs for polymers, guest uptake is essentially due to only the amorphous phase and that, differently from the case of PPO, the crystalline phase of PPPO is not nanoporous.

It is worth adding that annealing procedures on both amorphous and semicrystalline samples, which do not alter significantly their degree of crystallinity, can largely reduce the

pollutant uptake. For instance, gravimetric CCl_4 sorption isotherms, of the amorphous and semicrystalline powders of curves A and B, after treatment at 220 °C (i.e., glass transition temperature of PPPO⁴⁸) for 240 min (reported as A' and B' curves, with empty symbols and dotted curves in Figure 2), show a reduction of the guest uptake of roughly 40%. This reduction of pollutant uptake is due to the expected densification of the amorphous phases, occurring by thermal treatments close to T_g .^{51,52}

Hence, our results indicate that the free volume of PPPO amorphous phases is largely dependent on the preparation procedure as well as on the thermal history and thus important differences of the guest uptakes may be observed in amorphous PPPO samples.

3.2. PPPO-Based Monolithic Aerogels. Physically cross-linked aerogels are generally prepared by scCO_2 extraction of thermoreversible physically cross-linked gels.^{32–47} PPPO is easily dissolved in many organic solvents (e.g., CHCl_3 , CH_2Cl_2 , benzene) but all our attempts to obtain gelification on cooling, at least for polymer concentrations ≤ 10 wt %, were unsuccessful.

Unlike PPPO, syndiotactic polystyrene can readily form strong elastic thermoreversible gels^{53,54} in many solvents⁵⁵ and highly stereoregular s-PS can form thermoreversible gels for concentrations as low as $C_{\text{pol}} = 1$ wt %.⁵⁶ Thus, thermoreversible gels with PPPO can be also easily obtained for blends with syndiotactic polystyrene (s-PS), even for PPPO/s-PS ratios as high as 90/10 (Figure 3A). Moreover, as already observed for

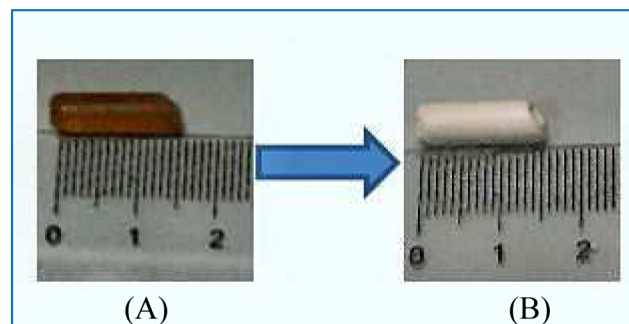


Figure 3. Photographs of (A) a cylindrical 90/10 PPPO/s-PS gel, with $C_{\text{pol}} = 10$ wt % and (B) the corresponding monolithic aerogel, with porosity $P = 90\%$ as obtained by scCO_2 drying.

PPPO/s-PS gels,⁴⁵ robust monolithic aerogels with good handling characteristics can be easily obtained from the mixed PPPO/s-PS gels by sudden solvent extraction by scCO_2 (Figure 3B).

Scanning electron microscopy (SEM) images of a 50/50 PPPO/s-PS aerogel are shown in Figure 4.

The SEM images clearly show that as previously observed for PPO/s-PS aerogels,⁴⁵ the typical fibrillar morphology of s-PS aerogels^{40,55,56} is maintained in PPPO/s-PS aerogels while PPPO beads with diameter of 0.5–1 μm included in the fiber network can be also observed. Thus, we can assume that the maintenance of the s-PS fibrillar morphology allows the obtaining of robust monolithic PPPO/s-PS aerogels with good handling characteristics.

X-ray diffraction patterns of aerogels obtained from physical gels of s-PS and of 50/50 and 90/10 PPPO/s-PS blends, in CHCl_3 and with polymer concentration $C_{\text{pol}} = 10$ wt %, are reported in Figure 5.

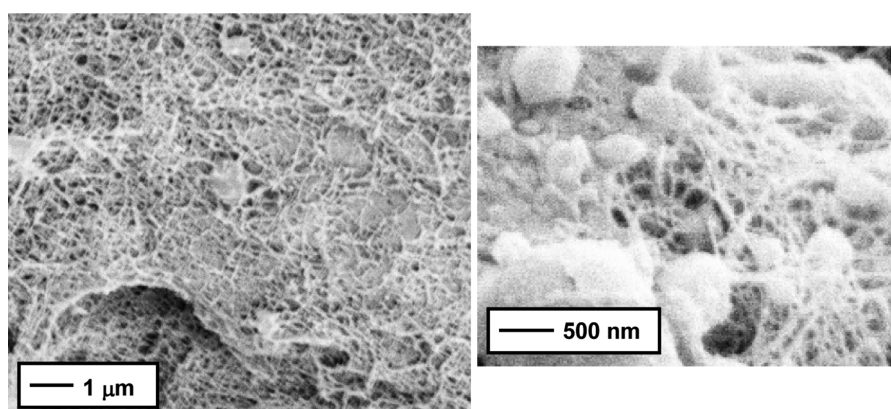


Figure 4. SEM images of a PPPO/s-PS aerogel with porosity $P = 90\%$ obtained from a 50/50 PPPO/s-PS gel prepared in chloroform with $C_{\text{pol}} = 10$ wt %, after complete solvent extraction by scCO_2 .

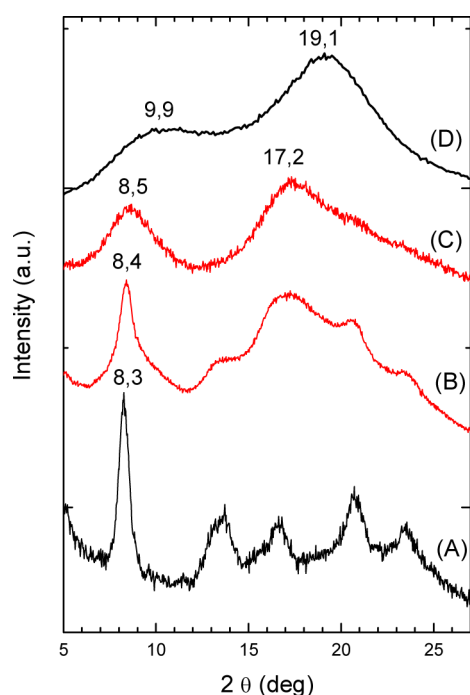


Figure 5. X-ray diffraction patterns ($\text{CuK}\alpha$ radiation) of aerogels as obtained by scCO_2 extraction of gels in chloroform, with $C_{\text{pol}} = 10$ wt %, of (A) s-PS (nanoporous-crystalline δ form) (B) s-PS/PPPO, 50/50 by wt; (C) s-PS/PPPO, 10/90 by wt. (D) For the sake of comparison, the diffraction of an amorphous sample of s-PS is also shown.

The 50/50 PPPO/s-PS aerogel (Figure 5B) presents, besides other broader peaks, a diffraction peak at $2\theta = 8.3^\circ$ corresponding to the 010 reflection of the nanoporous δ phase of s-PS (Figure 4A).²³ The 90/10 PPPO/s-PS aerogel (Figure 5C) only shows two broad amorphous halos, whose maxima are slightly shifted to lower 2θ values (8.5 and 17.2°), also with respect to the high-free-volume PPPO amorphous powder of Figure 1B. A comparison with the X-ray diffraction pattern of an amorphous s-PS film,^{57,58} presenting the typical halos roughly centered at $2\theta \approx 10^\circ$ and 20° (Figure 5D), clearly indicates that this shift toward lower angles of the amorphous halos of PPPO is not due to the s-PS blend component.

Adsorption–desorption N_2 isotherms (where the sorption is expressed as cm^3 of nitrogen in normal conditions per gram of polymer), for the aerogels of Figure 5A–C are compared with those of the PPPO commercial semicrystalline powder, in

Figure 6. The corresponding values for the total surface areas S_{BET} and total pore volume V_{tot} are compared in Table 1.

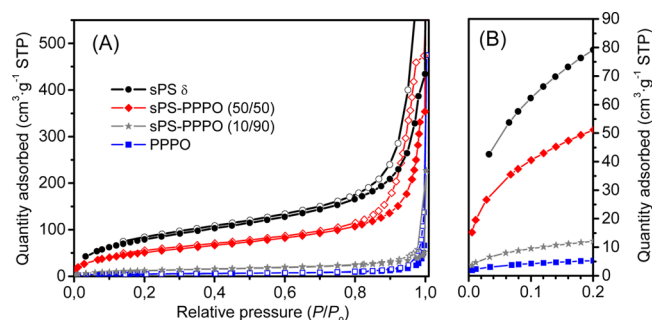


Figure 6. (A) Volumetric N_2 adsorption isotherms recorded at 77 K of the commercial Tenax powder (blue squares) and of aerogels of s-PS/PPPO 10/90 by wt (gray stars), s-PS/PPPO 50/50 by wt (red diamonds), and s-PS (nanoporous δ crystalline form) (black circles). Filled and empty scatters refer to the adsorption and desorption branches, respectively. (B) Detail of the adsorption branch, for low pressures.

Table 1. Total Surface Area (S_{BET}) and Total Pore Volume (V_{tot}) of Aerogels and Powders Based on s-PS and PPPO

| samples | polymer composition (w/w) | S_{BET}^a ($\text{m}^2 \text{g}^{-1}$) | V_{tot}^b ($\text{cm}^3 \text{g}^{-1}$) |
|-----------------------|---------------------------|---|--|
| aerogels ^c | s-PS(δ -form) | 290 | 0.31 |
| | PPPO/s-PS, 50/50 | 197 | 0.20 |
| | PPPO/s-PS, 90/10 | 47 | 0.04 |
| powders | s-PS(δ -form) | 43 | 0.10 |
| | PPPO | 20 ^d | 0.02 |

^aTotal area evaluated following the BET model in the standard $0.05 < p/p_0 < 0.25$ pressure range. ^bTotal pore volume calculated as volume of the liquid at $p/p_0 \approx 0.90$. ^cAs prepared from chloroform gels with a same polymer content ($C_{\text{pol}} = 10$ wt %). ^dIt is worth noting that as already reported in ref 6, the measured specific surface area of PPPO is lower than the advertised value of $35 \text{ m}^2/\text{g}$.

It is apparent from Table 1 that both S_{BET} and V_{tot} largely increase moving from powders to aerogels. Relevant is the increase of the surface area, by factors of roughly 2.3 and 10 moving from the PPPO powder to the 90/10 and 50/50 aerogels, respectively (3rd column of Table 1). This increase is due to the s-PS δ -form, which is characterized by nanopores having the same volume of ca. 115 \AA^3 .²⁴

CCl_4 sorption isotherms, at 35 °C and for p/p_0 up to 0.20, are reported in Figure 7, for the aerogels of Figure 5 and

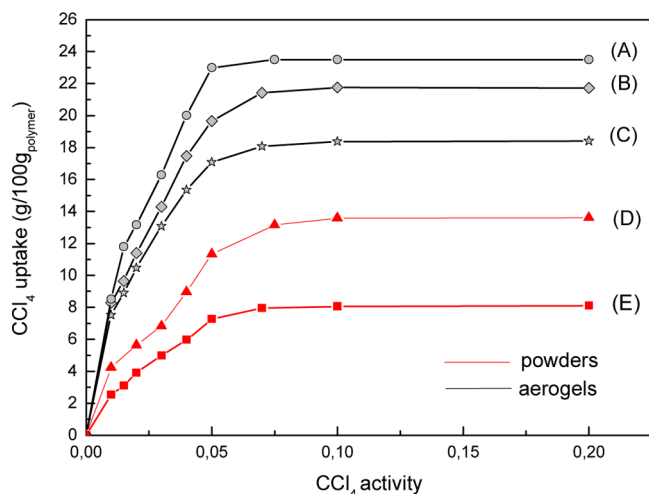


Figure 7. CCl_4 sorption isotherms at 35 °C for the aerogels of Figure 3A–C: (A) s-PS, δ form; (B) PPPO/s-PS 50/50 wt % (C) PPPO/s-PS 90/10 wt %. For the sake of comparison, the sorption isotherms of the (D) highly sorbent PPPO amorphous and (E) semicrystalline powders of Figure 2 are replotted.

compared with those of the PPPO powders of Figure 2. It is apparent that the PPPO/s-PS aerogels present CCl_4 uptake much higher than for the most efficient PPPO powders. This is only in part due to the higher sorption ability of the nanoporous δ form of s-PS (Figure 7A). In fact, the aerogel containing only 10% of s-PS (Figure 7C), which includes a negligible amount of nanoporous δ phase (as shown by the fully amorphous pattern of Figure 5C), presents a guest uptake roughly 30% higher than the best PPPO powder (Figure 7D).

Although the evaluated surface areas (Table 1) and the CCl_4 equilibrium uptakes (Figures 7) are markedly larger for aerogels than for powders, the sorption kinetics are similar. This is shown, for instance in Figure 8, for the sorption kinetics relative

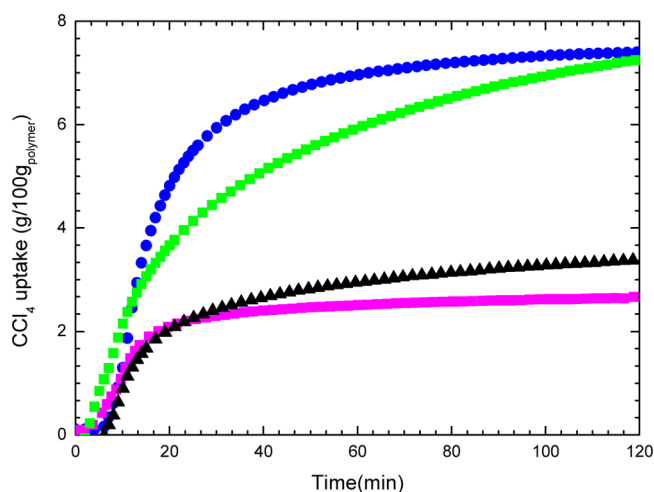


Figure 8. Sorption kinetics relative to a sudden increase of CCl_4 activity from zero up to $p/p_0 = 0.01$, for the PPPO/s-PS 90/10 wt % aerogel (blue circles), for δ -sPS aerogel (green squares), for PPPO amorphous powder (black triangles), and commercial PPPO semicrystalline powder (magenta squares).

to a sudden increase of CCl_4 activity from zero up to $p/p_0 = 0.01$. It is apparent that the monolithic 90/10 PPPO/s-PS aerogel (circles) maintains the fast sorption kinetics of fine powders (triangles and stars) with a half-time for the equilibrium lower than 15 min.

In this respect, it is worth adding that the monolithic s-PS aerogel (squares in Figure 8), which exhibits the highest surface area (Table 1) and the highest CCl_4 uptake (Figure 7), presents a half-time for the equilibrium higher than 20 min. This slower diffusivity of CCl_4 in s-PS samples can be easily rationalized on the basis of attractive interactions of CCl_4 molecules in the crystalline cavities of the δ form of s-PS, analogous to those studied in detail for other chlorinated organic guests.^{59–61}

The same aerogels have been compared as for their ability to remove pollutants being present in traces in water. For instance for PPPO/s-PS aerogels, the equilibrium uptake of CCl_4 and 1,2-dichloroethane (DCE) from 10 ppm aqueous solutions are reported in Figure 9, versus the PPPO weight percent. It is worth noting that both the shape and the dimensions of the aerogels were not modified when immersed in aqueous solutions.

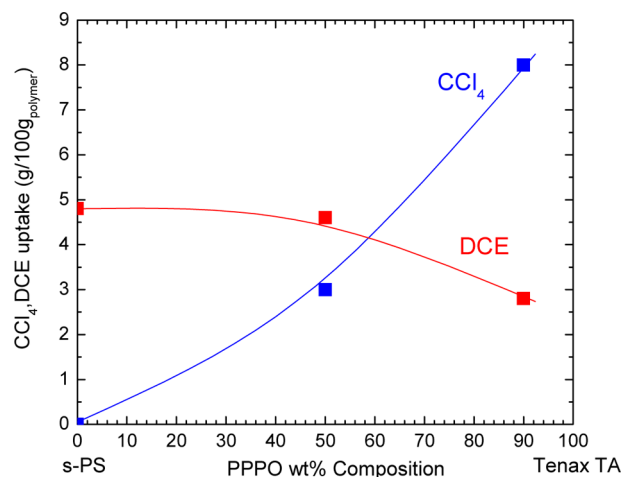


Figure 9. Equilibrium uptake (wt %) of CCl_4 and DCE from dilute aqueous solutions (10 ppm) for PPPO/s-PS aerogels (as obtained from gels with $C_{\text{pol}} = 10$ wt %) vs the PPPO wt % composition. PPPO rich aerogels are particularly suitable for removal of CCl_4 traces from diluted aqueous solutions. Continuous lines are guide for eyes.

The uptake of CCl_4 by the PPPO/s-PS, 90/10 aerogel is large (nearly 8 wt %) also higher than for the commercial powder (7 wt %) and much higher than for the s-PS aerogel. In fact, s-PS aerogels, which are highly efficient in the removal of other similar organic guests, like DCE⁴² (red curve in Figure 9) and in the removal of the same CCl_4 guest from vapor phase (Figures 7 and 8), absorb a negligible amount of CCl_4 from diluted aqueous solutions.

This is possibly due to the large hydration sphere^{62,63} of this symmetrical apolar molecule presenting highly polar C–Cl bonds, possibly exceeding the size of the crystalline cavity of the nanoporous δ crystalline phase (115 Å³).²⁴

4. CONCLUSIONS

Depending on the preparation procedure, fully amorphous PPPO samples with different amorphous halos indicating a different free volume can be obtained. The CCl_4 sorption measurements show that the guest uptake for fully amorphous

powders, as obtained by scCO_2 extraction of concentrated solutions, can be much higher than for commercial sorbent materials based on semicrystalline PPPO (Tenax). Annealing procedures on both amorphous and semicrystalline samples can largely reduce the pollutant uptake, due to the densification of the amorphous phases. Hence, the sorption ability of PPPO samples is largely dependent on their preparation procedure as well as on their thermal history.

The comparison of molecular sorption behavior of the considered PPPO samples also allows to conclude that, differently from the case of PPO and as generally occurs for polymers, the guest uptake is essentially due to its amorphous phase while its crystalline phase is not nanoporous.

Although PPPO does not form physical gels from diluted solutions, gels can be easily obtained for blends with syndiotactic polystyrene (s-PS), also for PPPO/s-PS ratios as high as 90/10. These mixed gels lead to robust monolithic aerogels by sudden solvent extraction by scCO_2 . SEM experiments suggest that the obtaining of PPPO/s-PS aerogels is due to the s-PS fibrillar morphology. The obtained aerogels exhibit fully amorphous PPPO with a high-free-volume amorphous phase. Moreover, s-PS rich (wt % > 50) aerogels exhibit, beside a high-free-volume PPPO amorphous phases, the highly sorbent nanoporous-crystalline δ phase of s-PS.

Monolithic PPPO/s-PS aerogels present many advantages as sorbent materials with respect to the commercially relevant PPPO powders. In fact, besides the obvious advantages in terms of easier and safer handling, the new monolithic aerogels generally present higher equilibrium guest uptake and maintain diffusivities similar to those of the powders. Volumetric N_2 adsorption isotherms show that the surface area (S_{BET}) increases in the aerogels with respect to the powders, by factors of roughly 2.3 and 10 for the monolithic 90/10 and 50/50 PPPO/s-PS aerogels. Particularly interesting is the CCl_4 uptake at low activities from the monolithic 90/10 PPPO/s-PS aerogel. In fact, the CCl_4 uptake from vapor phase at $p/p^\circ = 0.01$ (7.5 wt %) is nearly double than for the PPPO powders (in the range 2.5–4.5 wt %), whereas the uptake from diluted (10 ppm) aqueous solutions (8 wt %) is much higher than for the s-PS aerogel (<0.1%).

The observed increases of surface area and of guest uptakes in the aerogels, observed for the PPPO/s-PS aerogels with respect to the powders, are in part due the presence of the δ phase of s-PS and to its crystalline nanocavities and in part due to the less dense packing of the amorphous phase in the aerogels. The whole set of results indicates that monolithic PPPO-based aerogels are particularly suitable for efficient, easy, and safe removal of pollutants from water and air.

AUTHOR INFORMATION

Corresponding Author

*E-mail: cdaniel@unisa.it.

Author Contributions

The manuscript was written through contributions of all authors. All authors have given approval to the final version of the manuscript.

Notes

The authors declare no competing financial interest.

ACKNOWLEDGMENTS

We thank Dr. Paola Rizzo and Dr. Concetta D'Aniello of University of Salerno, Prof. Giuseppe Mensitieri and Dr.

Michele Galizia of University of Naples "Federico II", and Prof. Giuseppe Spoto of University of Turin for useful discussions. Dr. Stefano Cardea of Università degli Studi di Salerno is acknowledged for SEM measurements. Financial support of the "Ministero dell'Istruzione, dell'Università e della Ricerca" and of Regione Campania is gratefully acknowledged.

REFERENCES

- (1) Hay, A. S. U.S. Patent 3 432 466, March 11, 1969.
- (2) Van Wijk, R. J. *Chromatogr. Sci.* **1970**, *8*, 418–420.
- (3) Maier, I.; Fieber, M. J. *High Resolut. Chromatogr.* **1988**, *11*, 566–576.
- (4) Jens Laaks, J.; Jochmann, M. A.; Schilling, B.; Schmidt, T. C. *Anal. Chem.* **2010**, *82*, 7641–7648.
- (5) Kim, Y.-H.; Kim, K.-H. *Anal. Chem.* **2012**, *84*, 8284–8293.
- (6) Alfeeli, B.; Taylor, L. T.; Agah, M. *Microchem. J.* **2010**, *95*, 259–267.
- (7) Alfeeli, B.; Jain, V.; Johnson, R. K.; Beyer, F. L.; Heflin, J. R.; Agah, M. *Microchem. J.* **2011**, *98*, 240–245.
- (8) Dettmer, K.; Engewald, W. *Anal. Bioanal. Chem.* **2002**, *373*, 490–500.
- (9) Harper, M. J. *Chromatogr., A* **2000**, *885*, 129–151.
- (10) Oen, A. M. P.; Breedveld, G. D.; Kalaitzidis, S.; Christanis, K.; Cornelissen, G. *Environ. Toxicol. Chem.* **2006**, *25*, 1258–1267.
- (11) Barrero-Moreno, J. M.; Tirendi, S.; Reniero, F.; Giordano, G.; Kotzias, D. *Rapid Commun. Mass Spectrom.* **2008**, *22*, 471–476.
- (12) Leva, P.; Katsoyiannis, A.; Barrero-Morero, J.; Kephelopoulou, S.; Kotzias, D. *J. Environ. Sci. Health, Part B* **2009**, *44*, 51–57.
- (13) Daniel, C.; Longo, S.; Vitillo, J. G.; Fasano, G.; Guerra, G. *Chem. Mater.* **2011**, *23*, 3195–3200.
- (14) Tarallo, O.; Petraccone, V.; Daniel, C.; Fasano, G.; Rizzo, P.; Guerra, G. *J. Mater. Chem.* **2012**, *22*, 11672–11680.
- (15) Galizia, M.; Daniel, C.; Fasano, G.; Guerra, G.; Mensitieri, G. *Macromolecules* **2012**, *45*, 3604–3615.
- (16) Daniel, C.; Zhovner, D.; Guerra, G. *Macromolecules* **2013**, *46*, 449–454.
- (17) Factor, A.; Heinsohn, G. E.; Vogt, L. H., Jr. *J. Polym. Sci., Polym. Lett. Ed.* **1969**, *7*, 205–209.
- (18) Ilinitch, O. M.; Semin, G. L.; Chertova, M. V.; Zamaraev, K. I. *J. Membr. Sci.* **1992**, *66*, 1–8.
- (19) Aguilar-Vega, M.; Paul, D. R. *J. Polym. Sci., Part B: Polym. Phys.* **1993**, *31*, 1577–1589.
- (20) Alentiev, A.; Drioli, E.; Gokzhaev, M.; Golemme, G.; Ilinitch, O. M.; Lapkin, A. A.; Volkov, V.; Yampolskii, Yu. *J. Membr. Sci.* **1998**, *138*, 99–107.
- (21) Khulbe, K. C.; Matsuura, T.; Lamarche, G.; Lamarche, A. -M. *J. Membr. Sci.* **2000**, *170*, 81–89.
- (22) Sterescu, D. M.; Stamatialis, D. F.; Mendes, E.; Kruse, J.; Rätzke, K.; Faupel, F.; Wessling, M. *Macromolecules* **2007**, *40*, 5400–5410.
- (23) De Rosa, C.; Guerra, G.; Petraccone, V.; Pirozzi, B. *Macromolecules* **1997**, *30*, 4147–4152.
- (24) Milano, G.; Venditto, V.; Guerra, G.; Cavallo, L.; Ciambelli, P.; Sannino, D. *Chem. Mater.* **2001**, *13*, 1506–1511.
- (25) Petraccone, V.; Ruiz de Ballesteros, O.; Tarallo, O.; Rizzo, P.; Guerra, G. *Chem. Mater.* **2008**, *20*, 3663–3668.
- (26) Guerra, G.; Manfredi, C.; Musto, P.; Tavone, S. *Macromolecules* **1998**, *31*, 1329–1334.
- (27) Musto, P.; Mensitieri, G.; Cotugno, S.; Guerra, G.; Venditto, V. *Macromolecules* **2002**, *35*, 2296–2304.
- (28) Pierre, A. C.; Pajonk, G. M. *Chem. Rev.* **2002**, *102*, 4243–4265.
- (29) Pekala, R. W. *J. Mater. Sci.* **1989**, *24*, 3221–3227.
- (30) Choi, S.-J.; Kwon, T.-H.; Im, H.; Dong-Il Moon, D.-I.; Baek, D. J.; Myeong-Lok Seol, M.-L.; Duarte, J. P.; Choi, Y.-K. *ACS Appl. Mater. Interfaces* **2011**, *3*, 4552–4556.
- (31) Meador, M. A. B.; Malow, E. J.; Silva, R.; Wright, S.; Quade, D.; Vivod, S. L.; Guo, H.; Guo, J.; Cakmak, M. *ACS Appl. Mater. Interfaces* **2012**, *4*, 536–544.

- (32) Beaucage, G.; Aubert, J. H.; Lagasse, R. R.; Schaefer, D. W.; Rieker, T. P.; Erlich, P.; Stein, R. S.; Kulkarni, S.; Whaley, P. D. *J. Polym. Sci., Part B: Polym. Phys.* **1996**, *34*, 3063–3072.
- (33) Cardea, S.; Gugliuzza, A.; Sessa, M.; Aceto, M. C.; Drioli, E.; Reverchon, E. *ACS Appl. Mater. Interfaces* **2009**, *1*, 171–180.
- (34) Daniel, C.; Vitillo, J. G.; Fasano, G.; Guerra, G. *ACS Appl. Mater. Interfaces* **2011**, *3*, 969–977.
- (35) Guenet, J. M.; Parmentier, J.; Daniel, C. *Soft Mater.* **2011**, *9*, 280–294.
- (36) Peterson, G. R.; Cychosz, K. A.; Thommes, M.; Hope-Weeks, L. *J. Chem. Commun.* **2012**, *48*, 11754–11756.
- (37) Robitzner, M.; David, L.; Rochas, C.; Di Renzo, F.; Quignard, F. *Langmuir* **2008**, *24*, 12547–12552.
- (38) Quignard, F.; Valentin, R.; Di Renzo, F. *New J. Chem.* **2008**, *32*, 1300–1310.
- (39) Ding, B.; Cai, J.; Huang, J.; Zhang, L.; Chen, Y.; Shi, X.; Du, Y.; Kuga, S. *J. Mater. Chem.* **2012**, *22*, 5801–5809.
- (40) Daniel, C.; Alfano, D.; Venditto, V.; Cardea, S.; Reverchon, E.; Larobina, D.; Mensitieri, G.; Guerra, G. *Adv. Mater.* **2005**, *17*, 1515–1518.
- (41) Guerra, G.; Mensitieri, G.; Venditto, V.; Reverchon, E.; Daniel, C. PCT Int. Appl. 2005, WO 2005012402.
- (42) Malik, S.; Roizard, D.; Guenet, J.-M. *Macromolecules* **2006**, *39*, 5957–5959.
- (43) Daniel, C.; Sannino, D.; Guerra, G. *Chem. Mater.* **2008**, *20*, 577–582.
- (44) Daniel, C.; Giudice, S.; Guerra, G. *Chem. Mater.* **2009**, *21*, 1028–1034.
- (45) Daniel, C.; Longo, S.; Cardea, S.; Vitillo, J. G.; Guerra, G. *RSC Adv.* **2012**, *2*, 12011–12018.
- (46) Wang, X.; Jana, S. C. *Polymer* **2013**, *54*, 750–759.
- (47) Daniel, C.; Longo, S.; Ricciardi, R.; Reverchon, E.; Guerra, G. *Macromol. Rapid Commun.* **2013**, DOI: 10.1002/marc.201300260.
- (48) Brunauer, S.; Emmett, P. H.; Teller, E. *J. Am. Chem. Soc.* **1938**, *60*, 309–319.
- (49) Wrasidlo, W. *Macromolecules* **1971**, *5*, 642–648.
- (50) Agency for Toxic Substances and Disease Registry (ATSDR) *Toxicological Profile for Carbon Tetrachloride*.
- (51) Chan, A. H.; Paul, D. R. *J. Appl. Polym. Sci.* **1979**, *24*, 1539–1550.
- (52) Chan, A. H.; Paul, D. R. *Polym. Eng. Sci.* **1980**, *20*, 87–94.
- (53) Daniel, C.; Dammer, C.; Guenet, J. -M. *Polymer* **1994**, *35*, 4243–4246.
- (54) Daniel, C.; Alfano, D.; Guerra, G.; Musto, P. *Macromolecules* **2003**, *36*, 1713–1716.
- (55) Daniel, C.; Avallone, A.; Guerra, G. *Macromolecules* **2006**, *39*, 7578–7582.
- (56) Daniel, C.; Guerra, G. *ACS Symp. Ser.* **2010**, *1061*, 131–147.
- (57) Guerra, G.; Vitagliano, V. M.; De Rosa, C.; Petraccone, V.; Corradini, P. *Macromolecules* **1990**, *23*, 1539–1544.
- (58) Sago, T.; Itagaki, H.; Asano, T. *Soft Mater.* **2011**, *9*, 199–223.
- (59) Guerra, G.; Milano, G.; Venditto, V.; Musto, P.; De Rosa, C.; Cavallo, L. *Chem. Mater.* **2000**, *12*, 363–368.
- (60) Tamai, Y.; Tsujita, Y.; Fukuda, M. *J. Mol. Struct.* **2005**, *739*, 33–40.
- (61) Milano, G.; Guerra, G. *Progr. Mater. Sci.* **2009**, *54*, 68–88.
- (62) Sampson, J. E.; Blankenship, F. *Proc. Okla. Acad. Sci.* **1948**, *28*, 112–113.
- (63) Kaloustian, J.; Rosso, J. C.; Caranoni, C.; Carbonnel, L. *Rev. Chim. Miner.* **1976**, *13*, 334–342.